Journal of The Institute of Electronics and Information Engineers Vol.54, NO.5, May 2017 https://doi.org/10.5573/ieie.2017.54.5.11
ISSN 2287-5026(Print) / ISSN 2288-159X(Online)

논문 2017-54-5-2

RF MOSFET의 주파수 종속 입력 저항에 대한 이론적 분석

(Theoretical Analysis of Frequency Dependent Input Resistance in RF MOSFETs)

안 자 현*, 이 성 현**

(Jahyun Ahn and Seonghearn Lee©)

요 약

RF MOSFET에서 관찰된 입력 저항의 주파수 종속 특성이 단순화된 입력 등가회로로부터 유도된 pole과 zero 주파수 수식을 사용하여 자세히 분석되었다. 이러한 이론적 분석을 사용하여 저주파에서 입력저항의 감소현상이 포화영역에서 소스와 pinch-off 영역 사이의 채널저항으로부터 발생되는 것을 발견하였다. 이와 같이 저주파에서 입력저항이 감소하는 채널 저항 효과는 채널저항을 변화시키면서 소신호 등가회로 모델링을 수행하여 물리적으로 입증되었다.

Abstract

The frequency dependent input resistance observed in RF MOSFETs is analyzed in detail by deriving pole and zero frequency equations from a simplified input equivalent circuit. Using this theoretical analysis, we find that the reduction effect of the input resistance in the low frequency region arises from the channel resistance between source and pinch-off region in the saturation region. This channel resistance effect on the low frequency reduction of the input resistance is physically validated by performing small-signal equivalent circuit modeling with varying the channel resistance.

Keywords : MOSFET, CMOS, input resistance, RF modeling, frequency dependence

I. Introduction

S-parameters in two-port measurement system are widely used to develop a MOSFET equivalent circuit model and design RF integrated circuits (ICs), but it is very hard to analyze the frequency response of input resistance R_{IN} converted from S_{11}-parameter with the load resistance of 50Ω connected in output port[1].

As Lg is scaled down to deep sub-micron, R_{IN} is increased by another component due to the output resistance connected to the drain in the saturation region[1~4]. In previous study[1], the gate finger number Nf dependent characteristics of low-frequency R_{IN} measured from S_{11}-parameter of multi-finger sub-micron MOSFETs have been analyzed. Recently, it has been reported that R_{IN} of a standard MOSFET is largely reduced with increasing frequency at low frequencies[1~2]. Since this frequency dependence of R_{IN} has a decisive impact on the RF input characteristics of MOSFETs, its accurate modeling is very important for an input matching circuit design in RF ICs. However, this low frequency reduction phenomenon of R_{IN} has not been analyzed and its physical origin has not been investigated yet.

Therefore, in this paper, we have derived pole and zero frequency equations of R_{IN} in 0.18μm standard multi-finger N-MOSFETs using a physical equivalent

* 학생회원, ** 정회원, 한국외국어대학교 전자공학과
(Department of Electronics Engineering, Hankuk University of Foreign Studies)
© Corresponding Author(E-mail : shlee@hufs.ac.kr)
※ 이 연구는 2016학년도 한국외국어대학교 교내학술연구비의 지원에 의하여 이루어진 것임.
Received ; December 1, 2016 Revised ; February 20, 2017
Accepted ; April 11, 2017

circuit model. Using these equations, an original model parameter for reducing R_{IN} in the low frequency region is clearly identified in detail.

Ⅱ. Measurement

N-MOSFETs with a multi-finger layout (the gate length L_g=0.18μm, the unit gate finger width W_u=10μm, the gate finger number Nf=16, 64) fabricated by a standard CMOS process were used in this work. S-parameters of these devices were measured using on-wafer RF probe up to 30GHz. We carried out a de-embedding process for removing RF probe pad and metal interconnection parasitic components from measured S-parameters[5~6].

Using measured S_{11}-parameter, R_{IN} is obtained by the real part of input impedance[1~2]:

$$R_{IN} = Z_o \cdot \left[\frac{1+S_{11}}{1-S_{11}}\right] \quad (1)$$

where Z_O is the characteristic impedance of R_O=50Ω.

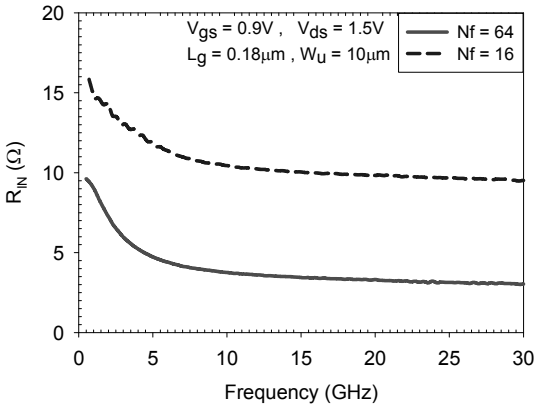

그림 1. Nf=16, 64 일 때 측정된 R_{IN}의 주파수 응답.
Fig. 1. The frequency response of measured R_{IN} for Nf=16 and 64.

Fig. 1 shows the frequency response of measured R_{IN} with a different Nf up to 30GHz using (1)[2]. In Fig. 1, R_{IN} is largely reduced by the pole frequency f_{pole} and flatted by the zero frequency f_{zero} at higher frequencies. The R_{IN} consists of the gate resistance R_g and the input resistance R'_{IN} seen behind R_g. Since R_g is independent of frequency, the frequency dependence in Fig. 1 is due to R'_{IN}. The high-frequency values of R_{IN} at Nf=64 are lower than those of Nf=16. This is because the frequency independent R_g included in R_{IN} is inversely proportional to Nf in a multi-finger gate layout. This reduction effect of R_{IN} versus frequency is analyzed in the next chapter by deriving the theoretical formula of f_{pole} and f_{zero}.

Ⅲ. Analysis

1. Input Resistance Equation

In order to obtain f_{pole} and f_{zero} equations of R_{IN}, we use a small-signal MOSFET equivalent circuit[7~9] with R_o=50Ω connected in output port for a S_{11}-parameter measurement setup in Fig. 2.

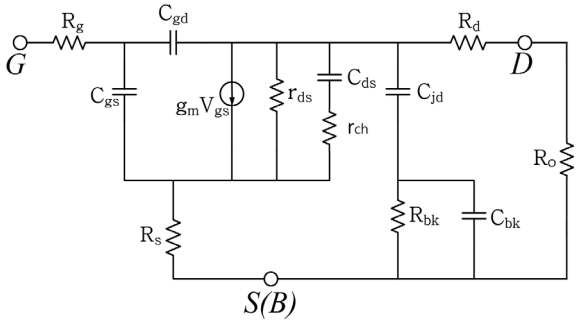

그림 2. S_{11}-parameter의 측정 setup에서 MOSFET 소신호 등가회로.
Fig. 2. A small-signal MOSFET equivalent circuit in a S_{11}-parameter measurement setup.

In this model, C_{gs} is the gate-source capacitance, C_{gd} is the gate-drain capacitance, g_m is the transconductance, r_{ds} is the differential drain-source resistance due to channel length modulation in the saturation region, C_{ds} is the depletion capacitance between drain and channel end in the saturation region, r_{ch} is the channel resistance between source and channel end in the saturation region[7], R_g is the gate resistance, R_d is the drain resistance, R_s is the source resistance, C_{jd} is the drain-bulk junction capacitance, R_{bk} is the bulk resistance, and C_{bk} is the bulk capacitance.

However, it is very difficult to derive f_{pole} and f_{zero} due to the complexity of Fig. 2. In order to simplify Fig. 2, the influence of junction and bulk parameters

(C_{jd}, C_{bk}, R_{bk}) on f_{pole} and f_{zero} is analyzed by using the following direct extraction method:

In the high-frequency(HF) region where the frequency dependence disappears, R_g, R_d, and R_s are extracted at V_{ds}=V_{gs}=0V using y-intercepts of $Re(Z_{11}-Z_{12})$, $Re(Z_{22}-Z_{12})$ and $Re(Z_{12})$ versus ω^{-2}, respectively[10]. C_{jd}, R_{bk} and C_{bk} are extracted using the following direct extraction method using Y-parameter equations[7, 11].

In order to check the influence of junction and bulk parameters, de-embedded R_{IN} is obtained by subtracting extracted values of R_d, C_{jd}, R_{bk} and C_{bk} from measured S-parameters[12]. Fig. 3 shows a comparison between de-embedded and measured R_{IN} vs. frequency. The de-embedded R_{IN} decreases in all frequency range, but these parameters have a very weak influence on f_{pole} and f_{zero} in Fig. 3. Thus, the physical reason for the low frequency reduction of R_{IN} in standard MOSFETs is not due to R_{bk}, unlike previous results in non-standard MOSFET[3~4].

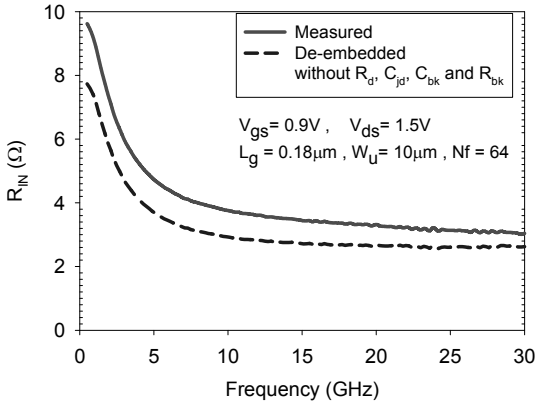

그림 3. 디임베딩된 R_{IN}과 측정된 R_{IN}의 주파수 응답.
Fig. 3. Frequency response of measured and de-embedded R_{IN}.

Thus, in order to reveal the physical origin of the reduction effect of R_{IN}, the frequency dependence of R_{IN} is analyzed using the simplified input equivalent circuit neglecting C_{jd}, R_{bk} and C_{bk} in Fig. 4 where the negative feedback resistance R_s is absorbed in the following formulas of C'_{gs}, C'_{ds}, g'_m and r'_{ds} by combining with C_{gs}, C_{ds}, g_m and r_{ds}[3~4]:

$$C'_{gs} = C_{gs}/(1+g_m R_s) \tag{2}$$

$$C'_{ds} = C_{ds}/(1+g_m R_s) \tag{3}$$

$$g'_m = g_m/(1+g_m R_s) \tag{4}$$

$$r'_{ds} = r_{ds}(1+g_m R_s) \tag{5}$$

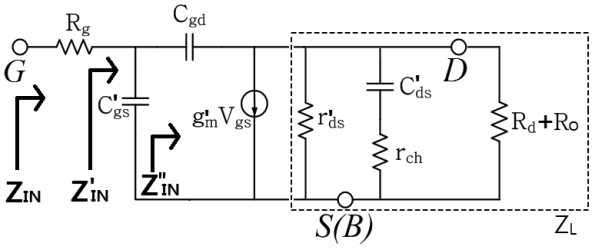

그림 4. C_{jd}, R_{bk}, C_{bk}가 무시되어 단순화된 입력 등가회로
Fig. 4. A simplified input equivalent circuit with neglecting C_{jd}, R_{bk} and C_{bk}.

In Fig. 4, Z'_{IN} is the input impedance seen in front of C'_{gs} and Z''_{IN} is one seen behind C'_{gs}. The effective load impedance Z_L in a dashed box is a circuit block with r'_{ds}, C'_{ds}, r_{ch} and R_o+R_d. From Fig. 4, Z''_{IN} is derived by:

$$Z''_{IN} = \frac{\frac{1}{jwC_{gd}} + Z_L}{g'_m Z_L + 1} \tag{6}$$

where Z_L is derived by:

$$Z_L = \frac{R_p + jwC'_{ds}R_p r_{ch}}{1 + jwC'_{ds}(R_p + r_{ch})} \tag{7}$$

where R_p is parallel block of r'_{ds} and R_d+R_o.

From Fig. 4, R'_{IN} is expressed by the real part of the parallel impedance Z'_{IN} of Z''_{IN} and C'_{gs}.

$$R'_{IN} = Re\left[\frac{\frac{1}{jwC'_{gs}}Z''_{IN}}{\frac{1}{jwC'_{gs}} + Z''_{IN}}\right] \tag{8}$$

Substituting (6) and (7) into (8), the following equation is derived:

$$R'_{IN} = \frac{A + Bw^2}{C + Dw^2 + Ew^4} \tag{9}$$

where

$$A = C_{gd}R_p(C_{gd} + C_{gd}R_p g'_m + C'_{ds}R_p g'_m)$$
$$B = w^2 C_{gd}^2 C'^2_{ds} R_p r_{ch}(R_p r_{ch} g'_m + r_{ch} + R_p)$$
$$C = [C'_{gs} + C_{gd}(1 + R_p g'_m)]^2$$
$$D = R_p^2(C'_{gs}C_{gd} + C_{gd}C'_{ds}r_{ch}g'_m + C'_{gs}C'_{ds} + C_{gd}C'_{ds})^2 + C'^2_{ds}r_{ch}[r_{ch}(C'_{gs} + C_{gd})^2 + 2R_p(C'_{gs}C_{gd}r_{ch}g'_m + C_{gd}^2 r_{ch}g'_m + (C'_{gs} + C_{gd})^2)]$$
$$E = (C'_{gs}C_{gd}C'_{ds}R_p r_{ch})^2$$

2. Pole and Zero Frequency

In order to derive f_{pole}, the denominator of (9) is divided by $\{C'_{gs}+C_{gd}(1+R_p g'_m)\}^2$ and then expressed by the following equation:

$$Den = 1 + aw^2 + bw^4 \tag{10}$$

where

$$a = [R_p^2(C'_{gs}C_{gd} + C_{gd}C'_{ds}r_{ch}g'_m + C'_{gs}C'_{ds} + C_{gd}C'_{ds})^2 + C'^2_{ds}r_{ch}(r_{ch}(C'_{gs} + C_{gd})^2 + 2R_p(C'_{gs}C_{gd}r_{ch}g'_m + C_{gd}^2 r_{ch}g'_m + (C'_{gs} + C_{gd})^2))]/(C'_{gs} + C_{gd}(1 + R_p g'_m))^2$$
$$b = (C'_{gs}C_{gd}C'_{ds}R_p r_{ch})^2/(C'_{gs} + C_{gd}(1 + R_p g'_m))^2$$

The equation of (10) can be rewritten by:

$$Den = (1 + pw^2)(1 + qw^2) \tag{11}$$

Solving a=p+q and b=pq obtained by (10) and (11), p is obtained by:

$$p = \frac{a + \sqrt{a^2 - 4b}}{2} \tag{12}$$

To calculate a and b in (12), intrinsic model parameters (C_{gs}, C_{gd}, C_{ds}, g_m, r_{ds} and r_{ch}) in Fig. 2 is extracted using intrinsic Y^i-parameter equations[7, 11] obtained by sequentially subtracting extracted values of R_d, C_{jd}, R_{bk}, C_{bk}, R_g, and R_s from measured S-parameters.

In order to eliminate the possible errors associated with the direct method, a small-signal equivalent circuit of Fig. 2 is optimized to fit the measured S-parameters as close as possible while parameters obtained from the direct method are used as initial values with narrow bounds. C'_{gs}, C'_{ds}, g'_m and r'_{ds} in Fig. 4 are determined using (2)-(5). Table 1 shows extracted model parameters, a and b of Nf=16 and 64.

Due to a >> b in Table 1, p ≈ a and p >> q. Thus, (11) is approximated by the following equation:

$$Den \approx 1 + aw^2 \tag{13}$$

Therefore, the dominant pole frequency f_{pole} is obtained by:

$$f_{pole} = \frac{1}{2\pi}\sqrt{\frac{(C'_{gs} + C_{gd}(1 + R_p g'_m))^2}{G^2 + H}} \tag{14}$$

where

$$G = R_p^2(C'_{gs}C_{gd} + C_{gd}C'_{ds}r_{ch}g'_m + C'_{gs}C'_{ds} + C_{gd}C'_{ds})^2$$
$$H = C'^2_{ds}r_{ch}(r_{ch}(C'_{gs} + C_{gd})^2 + 2R_p(C'_{gs}C_{gd}r_{ch}g'_m + C_{gd}^2 r_{ch}g'_m + (C'_{gs} + C_{gd})^2))$$

When a conventional equivalent circuit[2~4] without r_{ch} is used, f_{pole} using (14) at $r_{ch} = 0$ is calculated to be 43.03GHz at Nf=16 and 14.64GHz at Nf=64 which are much higher than measured ones in Fig. 1. However, using extracted r_{ch} in Table 1 to calculate (14), similar f_{pole} values to measured ones are obtained to be 3.78GHz at Nf=16 and 2.42GHz at Nf=64. These results clearly indicate that the low f_{pole} is due to r_{ch} in MOSFET.

표 1. MOSFET의 추출된 모델 파라미터, a와 b
Table1. Extracted model parameters, a and b of MOSFETs.

Parameter	Nf=16	Nf=64
R_g	3Ω	0.7Ω
R_d	3.4Ω	0.87Ω
r'_{ds}	414Ω	97Ω
r_{ch}	390Ω	65Ω
g'_m	0.0787S	0.31S
C'_{gs}	0.205pF	0.92pF
C_{gd}	0.063pF	0.250pF
C'_{ds}	0.1pF	0.85pF
a	1.77×10^{-21}	4.3×10^{-21}
b	2.2×10^{-45}	1.27×10^{-44}

From the numerator of (9), f_{zero} is derived by:

$$f_{zero} = \frac{1}{2\pi}\sqrt{\frac{C_{gd} + R_p g'_m(C_{gd} + C'_{ds})}{C_{gd}C'^2_{ds}r_{ch}(R_p r_{ch} g'_m + r_{ch} + R_p)}} \tag{15}$$

When a conventional equivalent circuit[3~4] without r_{ch} is used, f_{zero} using (15) doesn't exist. This completely disagrees with measured ones in Fig. 1. However, f_{zero} using extracted r_{ch} is calculated to be 6.04GHz at Nf=16 and 5.7GHz at Nf=64 which are similar to measured ones in Fig. 1.

Therefore, the large reduction phenomenon of R_{IN} in low frequency region under 5GHz in Fig. 1 originates from r_{ch} in denominators of (14) and (15).

Ⅳ. Verifications

In order to exactly prove the phenomenon of reducing R_{IN} due to r_{ch}, the frequency response of the R_{IN} is simulated with varying r_{ch} using Fig. 2. The modeled R_{IN} data at r_{ch} = 390Ω at Nf = 16 and r_{ch} = 65 Ω at Nf=64 agree well with measured ones up to 15GHz, verifying the accuracy of extracted model parameters. However, the modeling accuracy decreases in higher frequency range because of the frequency-dependent r_{ch} due to the vertically distributed RC effect in the saturation region[9].

In Fig. 5, when r_{ch} increases, R_{IN} is largely reduced and then flatted at lower frequencies because of reduction of the dominant f_{pole} and f_{zero}[12]. Also, the decreasing rate of R_{IN} increases when r_{ch} increases. This is a same tendency predicted in (14) and (15).

In this study, it is physically discovered that the reduction effect of R_{IN} at low frequency range in standard MOSFET is generated by low f_{pole} and f_{zero} due to channel resistance r_{ch} between source and pinch-off depletion region in the saturation region. Thus, it is very important that r_{ch} should be accurately extracted to model RF MOSFET equivalent circuit for RF IC design.

Ⅴ. Conclusion

The low frequency reduction effect of R_{IN} in RF MOSFETs using a standard CMOS process is analyzed in detail. In order to reveal the physical origin of this phenomenon, dominant f_{pole} and f_{zero} equations are derived from a simplified input equivalent circuit for the measurement of S_{11}-parameter.

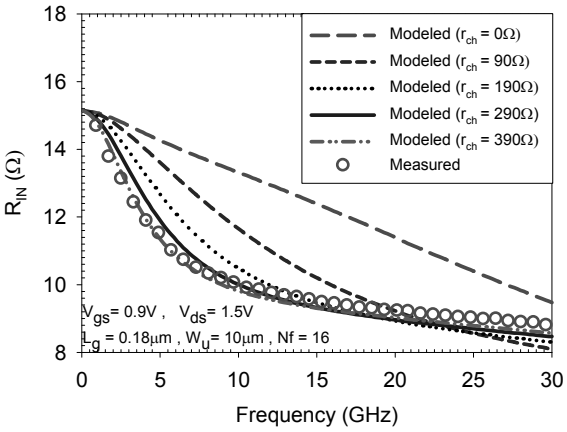

(a)

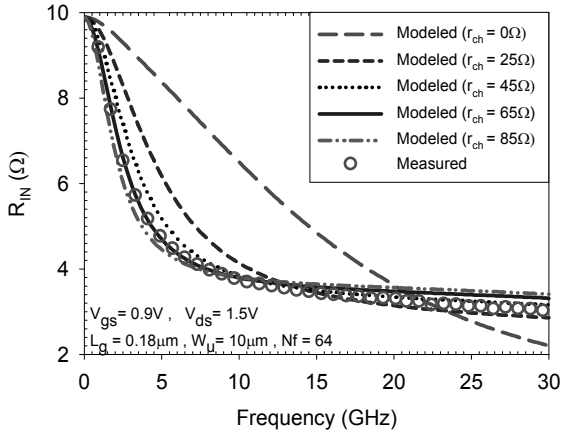

(b)

그림 5. 여러 가지 r_{ch}에 따라 모델된 R_{IN}과 측정된 R_{IN}의 주파수 응답.
(a) Nf=16
(b) Nf=64

Fig. 5. The frequency response of modeled and measured R_{IN} with various r_{ch}.
(a) Nf=16
(b) Nf=64

Based on these equations, it is physically found that the large reduction of R_{IN} at the low frequency range is generated from r_{ch} in the saturation region. The effect of r_{ch} on the low frequency dependence of R_{IN} is also verified by simulating an input equivalent circuit model with varying r_{ch}. Thus, a MOSFET equivalent circuit with r_{ch} should be accurately modeled to predict the frequency dependence of R_{IN} in standard RF MOSFETs.

REFERENCES

[1] J. Ahn and S. Lee, “Measurement and analysis of gate finger number dependence of input resistance for sub-micron MOSFETs,” J. Institute of Electronics and Information Engineers, vol. 51, no. 12, pp. 2695-2701, Dec. 2014.

[2] J. Ahn and S. Lee, “Analysis of kink phenomenon in S_{11}-parameter of standard RF MOSFETs,” Electron. Lett. vol. 51, no. 18, pp. 1453-1455, Sep. 2015.

[3] Y. S. Lin, “An analysis of small-signal source body resistance effect on RF MOSFETs for low-cost system-on-chip (SoC) applications,” IEEE Trans. Electron Devices, vol. 52, no. 7, pp. 1442-1451, July 2005.

[4] Y. S. Lin and S. S. Lu, “An analysis of small-signal gate-drain resistance effect on RF power MOSFETs,” IEEE Trans. Electron Devices, vol. 50, no. 2, pp. 525-528, Feb. 2003.

[5] J. Cha, J. Cha and S. Lee, “Uncertainty analysis of two-step and three-step method for de-embedding on-wafer RF transistor measurements,” IEEE Trans. Electron Devices, vol. 55, no. 8, pp. 2195-2201, Aug. 2008.

[6] J.-Y. Kim, M.-K. Choi, and S. Lee, “A thru-short-open de-embedding method for accurate on-wafer RF measurements of nano-scale MOSFETs,” J. Semicond. Technol. Sci., Vol. 12, No. 1, pp. 53-58, Mar., 2012.

[7] S. Hong and S. Lee, “Physical origin of gate voltage-dependent drain-source capacitance in short-channel MOSFETs,” Electron. Lett. vol. 50, no. 24, pp. 1879-1881, Nov. 2014.

[8] S. Hong and S. Lee, “Large-signal output equivalent circuit modeling for RF MOSFET IC simulation,” J. Semicond. Technol. Sci., vol. 15, no. 5, pp. 485-489, 2015

[9] S. Hong and S. Lee, “Improved high-frequency output equivalent circuit modelling for MOSFETs,” Electron. Lett., vol. 51, no. 24, pp. 2045-2047, Nov. 2015.

[10] S. Lee, “Accurate RF extraction method for resistances and inductances of sub-0.1 μm CMOS transistors,” Electron. Lett., vol. 41, no. 24, pp.1325-1327, Nov., 2005.

[11] Y. Lee, M. Choi, J. Koo, and S. Lee, “Bias and gate-length dependent data extraction of substrate circuit parameters for deep submicron MOSFETs,” Journal of The Institute of Electronics Engineers of Korea - Semiconductor and Devices, vol. 41, no. 12, pp. 27-34, 2004.

[12] J. Ahn and S. Lee, “Frequency-Dependence Analysis of RF Input Resistance for Multi-Finger Power MOSFETs,” in Proc. of 2014 IEIE Fall Conference, pp. 65-66, Nov. 2014.

저 자 소 개

안 자 현(학생회원)

2014년 한국외국어대학교 전자공학과 학사 졸업.

2014년 ~ 현재 한국외국어대학교 전자정보공학과 석사과정.

<주관심분야 : RF CMOS 소자 모델링>

이 성 현(정회원)-교신저자

1985년 고려대학교 전자공학과 학사 졸업.

1989년 미국 University of Minnesota 전기공학과 석사 졸업.

1992년 미국 University of Minnesota 전기공학과 박사 졸업.

1992 ~ 1995년 한국전자통신연구원 선임연구원

1995년 ~ 현재 한국외국어대학교 전자공학과 교수

<주관심분야 : CMOS 및 바이폴라 소자 모델링>